7

Ultrasonic Measurement and Imaging with Lateral Modulation – Echo, Tissue Motion and Elasticity

Chikayoshi Sumi
Sophia University
Japan

1. Introduction

It is remarkable that the pathological state of human soft tissues highly correlates with static and low-frequency mechanical properties, particularly shear elasticity (e.g., Sumi, 2005d). Accordingly, we have been developing ultrasonic (US)-strain-measurement-based one-dimensional (1D) (Sumi et al., 1993, 1995a, 2010f; Sumi, 1999b, 2005d, 2008a, 2010d; Sumi & Matsuzawa, 2007b), 2D (Sumi et al., 1993, 1995a; Sumi, 1999c, 2005d, 2006b, 2007g, 2008a, 2008c, 2010d) and 3D (Sumi, 1999c, 2005d, 2006b, 2007g, 2010d) shear or Young modulus reconstruction/imaging techniques as differential diagnostic tools for deseases of various *in vivo* tissues, such as the breast (Sumi, 1999a, 2005b, 2005d; Sumi & Matsuzawa 2007b; Sumi et al., 1995b(strain), 1996, 1997, 1999b, 2000b) and liver (Sumi et al., 2001a, 2001b; Sumi, 2005d), i.e., cancerous deseases etc. Other soft tissues such as heart or blood vessel are also our targets, i.e., myocardinal infraction, atherosclerosis etc. After the first report of the differential type inverse problem of shear modulus by Sumi (1993, 1995a), immediately the results obtained on agar phantoms [e.g., Sumi et al., 1994a(strain & shear modulus), 1994b, 1995d], *in vivo* breasts (e.g., Sumi et al., 1995b, 1996, 1997; Sumi, 1999a, 1999b) and *in vivo* liver (e.g., Sumi et al., 2000a, 2001a, 2001b; Sumi 2005d) were reported. For such *in vivo* tissues, a suitable combination of simple, minimally invasive therapy techniques such as chemotherapy, cryotherapy, and thermal therapy (e.g., Sumi, 2005d; Sumi et al., 2001a) etc with our reconstruction techniques would lead to an innovative, new clinical strategy that would enable differential diagnosis followed by immediate treatment so that overall medical expenses could be substantially reduced (Sumi, 2005d). This is because our developed techniques allow non-invasive confirming of a treatment effectiveness in real-time, i.e., a degeneration. Our early reports on the interstitial rf/micro wave thermal coagulation thrapy are Sumi et al., 2000a, 2001b; Sumi, 2005d, etc.

In the respective 1D, 2D and 3D techniques, a 1D (axial) displacement field, and 2D and 3D displacement vector fields generated by compression, vibration, heart motion, radiation force etc are measured to obtain 1D (axial) strain, and 2D and 3D strain tensor fields by partial differentiation. Many other researchers are also developing shear modulus reconstruction methods (e.g., Kallel & Bertrand, 1996; Plewes et al., 2000; Doyley et al., 2005) based on various displacement/strain measurement methods, e.g., conventional 1D Doppler method (Wilson & Robinson, 1982) and 1D autocorrelation method (1D AM) (Kasai et al.,

1985; Loupas et al., 1995) for blood flow measurement, and 1D (Ophir et al., 1991) or multidimensional (Yagi & Nakayama, 1988; Bohs & Trahey, 1991) crosscorrelation method (CCM). Now, various tissue motion and elasticity measurement/imaging have been performed over the world (see also references in Sumi et al., 2008i). In our case, other low frequency mechanical properties or quantities can also be reconstrcuted or measured, e.g., Poisson's ratio or Bulk modulus (Sumi, 2006b), density or inertia (Sumi, 2006b,2010d), viscoelasticity (e.g., Sumi, 2005d; Sumi et al., 2005a) and mechanical source (e.g., Sumi & Suekane, 2009e). Fluid such as blood is also our target (Sumi & Suekane, 2009e). These methods will also be used for a non-destructive evaluation, e.g., food engineering etc.

Previosuly, we reported a multidimensional phase matching method (Sumi et al., 1995d; Sumi, 1999a, 2008b) together with three novel methods of measuring *a multidimensional displacement vector* using a US signal phase, i.e., the multidimensional cross-spectrum phase gradient method (MCSPGM) (Sumi et al., 1995d; Sumi, 1999a, 2008b), multidimensional autocorrelation method (MAM) (Sumi, 2002c, 2005c, 2008b) and multidimensional Doppler method (MDM) (Sumi, 2002c, 2005c, 2008b). These methods can be applied to the measurement of the tissue strain tensor for above-mentioned shear modulus reconstruction (breast, liver, heart etc.), blood flow vector, sonar data, and other target motions. That is, the multidimensional phase matching allows coping with the decorrelation generated by out-of-motion from a beam or a 2D frame. Although the CCM requires the numerical interpolation of the crosscorrelation function using cosine, parabolic functions, etc to yield analogue displacement vector data, our developed multidimensional methods do not require such interpolation. That is, these methods require only sampled echo data and then do not suffer any artifact errors due to such interpolation. Specifically, in MCSPGM (Sumi et al., 1995d; Sumi, 1999a, 2008b), a local displacement vector is estimated using the local echo phase characteristics, i.e., from the gradient of the phase of the local cross-spectrum evaluated from the local region echo data. In contrast, the other two methods use an instantaneous US phase (Sumi, 2002c, 2005c, 2008b). By performing the multidimensional phase matching using a coarsely measured displacement data by a multidimensional cross-correlation method (MCCM) (Sumi et al., 1995d; Sumi, 1999a, 2008b) or MCSPGM using sampled echo data spatially thinned out (Sumi, 2005d, 2008b), all the methods enable *simultaneous* axial, lateral and elevational displacement measurements. The multidimensional phase matching method can cope with the decorrelation of local echo data and aliasing that occurs due to a large displacement, i.e., by searching for corresponding local echo data. Significantly, this phase matching method improves the measurement accuracies of multidimensional methods. As shown by simulations (Sumi, 2008b), the accuracies of the multidimensional displacement vector measurement methods are comparable; however, MAM and MDM require less computational time (particularly, MDM) than MCSPGM.

Generally, when using such displacement vector measurement methods, the measurement accuracy of lateral displacement was lower than that of axial displacement (Sumi et al, 1995d; Sumi, 1999a, 1999c, 2005c, 2008b; Sumi & Sato, 2007c; Sumi & Ebisawa, 2009a). Even if the target dominantly moves or becomes deformed in the lateral direction, our simultaneous measurements using the multidimensional phase matching result in the accurate measurement of axial displacement (Sumi, 2007f; Sumi et al., 1995b, 1995c). The multidimensional phase matching method also enabled us the high accuracy manual axial strain measurement (e.g., for breast, Sumi, 2005b, 2005d; Sumi & Matsuzawa, 2007b; Sumi et al., 1995b, 1996, 1997, 1999b, 2000b; liver, Sumi et al., 2001a, 2005d; others). By Sumi (1995b), the manual strain measurement was made possible by using multidimensional rf-echo

phase matching (cf. the first reports of shear modulus reconstrcution on *in vivo* beast, Sumi et al., 1996 and 1997; liver, Sumi et al., 2001b). Over the world, such an axial strain measurement/imaging by a manual axial compression using a US transducer has been clinically used. The modality is called as *Elastography* as named by Ophir (Ophir et al., 1991; Cespedes et al., 1993; Garra et al., 1997). Although the mesurement accuracy is significantly lower, some convetional 1D displacement measurement methods are also used instead of the multidimensional methods (e.g., Sumi 1999c; Sumi & Ebisawa, 2009a), i.e., ones originally used only for an axial displacement measurement along the axial direction. (e.g., Loupas at al., 1995; AM by Yamakawa & Shiina, 2001).

In our case, the measuement of axial strains generated by the axial compression or an arbitrary mechanical source are used for a multidimensional imaging of 1D reconstrcution (Sumi et al., 1993, 1995a, 2010f; Sumi, 1999c, 2005d, 2008a, 2010d; Sumi & Matsuzawa, 2007b). On the basis of the calculation of an axial strain ratio, several 1D reconstrcution methods were developed by Sumi. When the measurement accuracy of the axial strain is low, e.g., during thermal treatment (Sumi, 2005d; Sumi et al., 2001a), being dependent of the accuracy at each position, our developed *spatially-variant regularization* is performed for the strain measurement (Sumi & Sato, 2008c) or shear modulus reconstrcution (Sumi, 2008e; Sumi & Itoh, 2010e), i.e., an application of our developd implicit-integration (Sumi, 1998). That is, the measurement and reconstruction are stabilized to cope with the echo noise and strain measurement noise, respectively. For a focal lesion, by properly setting a reference region of shear modulus for the 1D reconsrcution, the 1D reconstruction allows yielding a higher contrast-to-noise ratio (CNR) than the axial strain (Sumi, 2005d; Sumi & Matsuzawa, 2007b; Sumi et al., 2010f). That is, the reference region should be set in the stress-concentrated or stress weak region in front of or behind the target stiff or soft lesion such that the reference region extends in the direction orthogonal to that of the dominant tissue deformation (Sumi, 2005b; Sumi & Matsuzawa, 2007b; Sumi et al., 1995d, 2010f). In addition, a mechanical source should be realized such that the target tissue deforms dominantly in a direction that extends in the direction of much shear-modulus varying (e.g. Sumi et al., 2010f). For the 1D strain measurement/imaging and 1D reconstruction, strain in the dominat deformation direction generated should be measured (e.g. Sumi & Ebisawa, 2009a). Moreover, for the practical imaging of 1D reconstruction, although human perception with respect to gray (negative or positive) scales and color scales must also be considered together with actual tissue shear modulus distributions, optimal displaying could be achieved by determining if the relative shear modulus or the inverse of the relative shear modulus should be imaged on the basis of their CNRs calculated using a stationary statistics of measured strains in the focal lesion and the surrounding region (Sumi et al., 2010f). Although the techniques for shear modulus reconstrcution methods including strain tensor calculations, multidimensional shear modulus reconstructions and the regularizations mentioned (Sumi, 1998, 2005d, 2006b, 2007g, 2008a, 2008e; Sumi & Sato, 2008c; Sumi & Itoh, 2010e) cannot be reviewed in detail in this chapter due to the limitation of the space, the important multidimensional phase matching is reviewed later (section 2.1).

However, if the lateral and elevational displacements can be measured with the same degree of an accuracy as that of the axial displacement, manual strain measurement and shear modulus reconstruction can be performed without considering the direction of the beam and target motion or mechanical source with the position (Sumi, 1999c, 2002a, 2002b, 2008a; Sumi et al., 2007e, 2008f, 2008i). That is, for an arbitrary mechanical source, 3D or 2D measurement/reconstruction with only attachment of the US transducer enables such

measurement and reconstruction. Clinically, such a measurement will enable the evaluation of the elasticity of more various tissues, e.g., under normal motion such as the heart, arm and leg muscles (during exercise) and even for the deep ROIs such as liver tissues, which are inaccessible from the body surface and normally deformed by heart motion or pulsation. Various possible configurations will increase the applications of the tissue motion measurement and mechanical property reconstrcutions.

For the blood flow vector measurement, a high accuracy displacement vector measurement had been performed (Jensen, 1998, 2001; Anderson, 1998, 2000) using a lateral oscillating method obtained by using Fraunhofer approximation (Steinberg, 1976; Goodman, 1996) together with some conventional 1D displacement measurement methods in respective axial and lateral directions, i.e., ones are originally used only for an axial displacement measurement along the axial direction. The measurement of blood flow in vessels running parallel to the surface of the body had been achieved. The method enabled the measurement of the lateral displacement/velocity that was more accurate than the use of the change in bandwidth (Newhouse, 1987).

The method falls in a category of the lateral modulation (LM) approach Sumi called (Sumi, 2002c, 2005c, 2005d). The LM was resolved by Sumi as the more simple beamforming that uses a coherent superimposition of steered, crossed beams (Sumi, 2002a, 2008a, 2008b; Sumi et al., 2008f, 2008i).

In the field of strain tensor measurement, the LM approach was applied first by Sumi (Sumi, 2004). For our tissue shear modulus reconstruction, to realize comparable high measurement accuracies of axial, lateral and elevational displacements, lateral and elevational modulation frequencies had to be significantly increased (Sumi, 2004, 2005c) compared with that observed in the reported application to the blood flow vector (Jensen, 1998, 2001; Anderson, 1998, 2000) and other tissue strain tensor (Liebgott et al., 2005) measurements (modulation frequency, 2.5 vs 1 mm^{-1}). This is because the strain tensor is obtained by differentiating the measured displacement vector components using a differential filter (i.e., a kind of high pass filter), the displacement vector must be measured with a considerable high accuracy. Deeply situated tissues must also be considered (e.g., liver). By Sumi (2005c, 2008b), a spherical focusing was obtained as a suitable focusing. Moreover, to increase the measurement accuracy, only a digital processing was used for obtaining plural multidimensional analytic signals (Sumi, 2002c, 2005c, 2008b). Moreover, it was confirmed that our developed LM methods are useful for imaging of the spatial difstribution of US reflectivity, i.e., echo imaging (Sumi, 2008a; Sumi et al., 2008f, 2008i). That is, a high resolution can be achieved in lateral and elevational directions as almost the same as that in the axial direction. Thus, it is expected that LM will lead to a next-generation US diagnosis equipped with various new modes such as displacement/velocity vector, strain tensor measrements and thier applications.

Although the LM methods developed by other groups (Jensen, 1998, 2001; Anderson, 1998, 2000; Liebgott, 2005) yield band-unlimited, modulated spectra by using infinite-length apodization functions (e.g., ringing-expressed by sinc functions), our developed lateral Gaussian envelope cosine modulation (LGECM) method realizes band-limited, modulated spectra, i.e., by using a finite length (not ringing) apodization function (Sumi, 2005c, 2008b). This does not cause aliasing. Moreover, for the blood flow vector measurement (Jensen, 1998, 2001; Anderson, 1998, 2000) and other strain tensor measuement (Liebgott et al., 2005), the respective measurements of axial and lateral displacements are performed using a conventional 1D displacement measurement method by realizing point spread functions

(PSF's) oscillating only in the lateral direction and only in the axial direction through a demodulation. Although we also developed a new accurate demodulation method only using digital signal processing (Sumi, 2010g), all the measurements suffer from the decorrelation of echo signals due to displacement orthogonal to the oscillation direction (Sumi, 2008b; Sumi & Shimizu, 2011). However, the highest accuracy in measuring target motions can be achieved by combined use (Sumi, 2002c, 2005c, 2008a, 2008b; Sumi et al., 2008f, 2008i) of the LM approach and our developed displacement vector measurement methods that enable *simultaneous* axial and lateral displacement measurements (Sumi et al., 1995d, 2002c; Sumi, 1999a, 2008b, 2005c). Not only our developed measurement increases the measurement accuracy of lateral displacements but also that of axial displacement (Sumi, 2005c, 2008b).

Our developed LM can be performed by superimposition of the simultaneously or successively transmitted/received, plural steered beams or frames with different steering angles obtained with the multiple transmission method (MTM, Sumi, 2002a, 2005d; Fox, 1978; Techavipoo, 2004). Alternatively, LM can also be realized from a set of received echo data (Sumi, 2008b; Sumi et al, 2008f, 2008i) using not a classical synthetic aperture but our previously developed multidirectional synthetic aperture method (MDSAM, e.g., Sumi, 2002a, 2005d; Tanter, 2002). That is, the aperture is synthesized in multidirections after receiving US signals. Because MDSAM requires less data acquisition time than MTM using successive US beam transmissions, if the transmitted US energies are sufficient, the beamforming suffers the less tissue motion artifact. To obtain high intensity transmitted US signals, a virtual source can be used (Sumi et al., 2010h). However, if tissue motion artifacts do not occur, MTM yields more accurate measurements. With this type of beamforming, multiple transducers can also be used (Sumi, 2008b; Sumi et al, 2008f, 2008i), e.g., when dealing with heart motion due to the existence of the obstacles such as bones. On the evaluations of statitics of measured strain tensor components and reconstructed relative shear modulus in a stiff inclusion of an agar phantom, accurate measurements and reconstructions were obtained (e.g., see Table I in Sumi, 2008f; Table VIII in Sumi, 2008i).

Alternatively, with MTM (Fox, 1978; Sumi, 2002a, 2005d; Techavipoo, 2004) and MDSAM (Sumi, 2002a, 2008b; Tanter, 2002), only the most accurately measured axial displacements from the respective beams obtained was used to obtain a displacement vector (i.e., there is no superimposition of beams). Although 1D measurement methods can also be used (Fox, 1978; Sumi, 2002a, 2005d; Tanter, 2002; Techavipoo, 2004) in place of the multidimensional measurement methods (Sumi, 2002a, 2008b), the same decorrelation of local echo signals (mentioned above) occurs due to target displacement in a direction orthogonal to the beams (Sumi et al., 1995d; Sumi, 2008b). Thus, the 1D measurement methods will result in a lower measurement accuracy than the corresponding multidimensional measurement methods, i.e., the 1D cross-spectrum phase gradient method (1D CSPGM) (Sumi et al., 1995d; Sumi, 1999a), conventional 1D AM (Kasai et al., 1985; Loupas et al., 1995), 1D DM (Sumi, 2008b), and 1D CCM (Ophir et al., 1991). Thus, not conventional 1D axial displacement measurement methods (e.g., 1D AM) but multidimensional displacement vector measurement methods should be used. Also for these beamformings, if necessary, separate plural transducers are also used simultaneously or successively.

However, under conditions in which motion artifacts do not occur, our previous comparison (Sumi, 2008b) of LM (or coherent superimposition) and non-superimposition methods by geometrical evaluations clarifies that the LM has the potential to yield more accurate measurements of axial and lateral displacements with less computational time.

However, for practical beamforming applications, the echo SNRs from steered beams must also be considered, i.e., an overly large steered angle makes the echo SNR low (Sumi et al., 2008i).

Moreover, LGECM method was improved using parabolic functions or Hanning windows instead of Gaussian functions in the apodization function. Hereafter, the new methods are respectively referred to as the parabolic modulation (PAM) method or Hanning modulation (HAM) method (Sumi, 2008a; Sumi et al., 2008i). Particularly, PAM enables decreases in effective aperture length (i.e., channels) and yield more accurate displacement vector measurements than LGECM. Although the Fourier transform of a parabolic function results in ringing effects, the new modulation yields no ringing effects in the spectra. PAM also yields a high spatial resolution in the reflectivity (echo) imaging with a high echo signal-to-noise ratio (SNR). Thus, we stop using the Fraunhofer approximation for LM. PAM is obtained on the basis of the *a priori* knowledge of the differences in the focusing scheme and shape between the parabolic function, Hanning window and Gaussian function, and the effects on the decays of the US signals during the propagation. That is, the US energy of the feet is lost during the US propagation and the main lobe contributes to echo signals, the mountains in the apodization functions should have a large full width at half maximum (FWHM) and short feet. Thus, we suceeded in a breakway from the Fraunhofer approximation (Sumi et al., 2006a).

Usually, for US imaging, US beam-forming parameters such as frequency, bandwidth, pulse shape, effective aperture size, and apodization function are designed and set appropriately. In addition, US transducer parameters such as the size and materials of the US array element used are also set appropriately. In determining such settings, the US properties of the target are also be considered (e.g., attenuation and scattering). Thus, all parameters are set appropriately for the consideration of a system that involves the US properties of the target. Previously, we proposed to set such parameters in order to realize the required PSF for LM on the basis of optimization theory by using the minimum norm least-squares estimation method (Sumi et al., 2006a; Sumi, 2007d, 2010a). The better envelope shape of the PSF than that of the PA is searched for on the basis of the knowledge of the ideal shape of PSF, i.e., having a large FWHM and short feet (e.g., Sumi et al., 2010c). Nonlinear optimization is also effective to yield such a proper PSF (Sumi et al., 2009c). Although conventional US beam-forming parameters are usually set on the basis of the experience of an engineer, our proposed method realizes the best possible beam-former using optimally determined parameters. Thus, spatial resolution and echo SNR are improved.

Although the optimized parameter can also be used, in this chapeter, PAM and LGECM are performed because they can be analytically obtained (Sumi et al., 2008i). As mentioned above, it was confirmed through simulations that when echo SNR is high (SNR ≈ 20 dB), MAM yields a higher accuracy measurement than MDM and vice versa (Sumi, 2008b). Here, the 2D demonstrations are shown on agar phantom that was statically compressed dominantly in a lateral direction (Sumi et al., 2008f), displacement of which cannot be accurately measured by a conventional beamforming. In addition, 2D shear modulus reconstrcutions are also shown together with strain tensor measurements.

In this chapeter, after reviewing our developed phase matching, PAM and LGECM, and MAM and MDM (section 2), the images and measurements obtained on an agar phantom are shown (section 3). Comparisons of the spatial resolution of the US images are made and the accuracies of the measured displacement vectors and elasticity (i.e., strain, shear modulus) are determined. Finally, discussions and future problems are provided with conclusions.

2. Brief reviews

2.1 Phase matching

To cope with the occurrence of decorrelation due to target motion and echo noise, we proposed the iterative phase matching method (Sumi et al., 1995d, 1999a, 2008b), i.e., the iterative search method for corresponding local region echo data. The search can be realized in spatial and spatial frequency domains using the estimate of the displacement vector obtained by a displacement vector measurement method or using *a priori* data of compression/stretching etc., i.e., by shifting echo data in a spatial domain or by multiplying a complex exponential by echo data in a spatial frequency domain using the estimate. First, this search method was used to increase the measurement accuracy of MCSPGM (e.g., Sumi et al., 1995d; Sumi, 1999a) using the estimate obtained by MCSPGM or MCCM. Here, we note that, strict echo compression/stretching can also be realized in the phase matching by setting a corresponding echo data in the local region using measured displacements and strains (Sumi, 2008b), whereas the effectiveness of the local echo compression/stretching is reported by Srinivasan et al. (2002). In the first phase matching, the estimate obtained at the adjacent point can be used to reduce the number of iterations of phase matching.

This phase matching method can also be used for MAM and MDM to increase measurement accuracy (Sumi, 2008b). That is, for MAM, this method enables the increase in the accuracy of instantaneous phase change and instantaneous spatial frequencies by improving the correlation of the local complex correlation function, whereas for MDM, this method enables the increase in their accuracy by increasing that of the temporal derivative in the Taylor expansion of the instantaneous phase of the complex signal. During the iterative phase matching, the moving-average width decreases as the local region size of MCSPGM decreases (Sumi, 1999a). This enables the increase in spatial resolution. Moreover, this increases the accuracy of strain measurement because the estimation accuracies of the instantaneous phase change and instantaneous spatial frequencies are improved due to their being not constant. If there exists no noise in echo data, the moving averaging is not needed and only phase matching should be performed. LM increases the convergence speed of the phase matching (Sumi, 2008b).

Thus, various applications of the actual axial strain measurements have been reported using axial (Cespedes et al., 1993; Garra et al., 1997) and multidimensional (Sumi et al., 1995b) displacement measurements, e.g., diagnosis of cancers of human *in vivo* breasts (Cespedes et al., 1993; Sumi et al., 1995b; Garra et al., 1997) and monitoring various low-invasive treatments such as interstitial rf/micro wave coagulation therapies of an *in vivo* liver carcinoma (Sumi et al., 2000a, 2001a, 2001b, 2005a, Sumi, 2002b, 2005d, 2007a). By Sumi (1995b), the manual strain measurement was made possible by using multidimensional rf-echo phase matching (Sumi et al., 1995d). These were achieved without any regularizations nor LMs.

However, reports of actual shear modulus reconstruction using measured strain tensor distributions are few with the exception of our reports (e.g., Sumi, 2007a, 2008a, 2008e; Sumi & Sato, 2008c; Sumi & Itoh, 2010e using the regularizations for strain measurement or shear modulus reconstrcution; Sumi, 2008a; Sumi et al., 2008f, 2008i using LM) and the reconstruction using a measured axial displacement distribution (e.g., Doyley et al., 2005 using another regularization for Young modulus). Specifically, we reported 2D direct shear modulus reconstruction using regularized strain tensor measurement (Sumi & Sato, 2008c; Sumi & Itoh, 2009b) as well as regularized direct 1D shear modulus reconstruction (Sumi, 2008e; Sumi & Itoh, 2010e; Sumi, 2007a) using raw strain tensor measurement. These

reconstructions were stably performed for agar phantoms by using our developed regularization, i.e., *spatially variant regularization* being dependent of the accuracies at each position of the measured strain tensor components. Because the measurement accuracy depends on the direction of the displacement, according to the accuracies of the respective displacements, they are also properly regularized, i.e., referred to as *displacement component-dependent regularization* or *directional-dependent regularization* (Sumi & Sato, 2008c; Sumi & Itoh, 2009b). As briefly reviewed in section 1, various 1D reconstructions using the axial strain were also obtained by Sumi for human *in vivo* tissues when the targets become deformed in the axial and lateral directions, respectively. By Sumi, in addition to the report (2008e), the regularizations were also performed (2005d; 2007a) for the strain measurement or shear modulus reconstrcution before, during and after the *in vivo* thermal coagulation treatment. However, simulations revealed that the 1D reconstrcutions such as strain ratio, implicit-integration etc lead to the inaccurate value of reconstrcution and geometrical artifact even if there exists no noise in the axial strain data used (Sumi, 2005d; Sumi & Matsuzawa, 2007b). Moreover, when the target deforms in the lateral direction, the 1D reconstruction further decreases the accuracy in reconstrcution (Sumi, 2007f). Moreover, for the 2D reconstruction, the use of only the regularizations still yields an inaccurate reconstruction (Sumi & Sato, 2008c; Sumi & Itoh, 2009b). Thus, LM was also used later (Sumi, 2008a; Sumi et al., 2008f, 2008i).

2.2 Complex signals with different single-octant and different single-quadrant spectra

Both the multidimensional autocorrelation method (MAM) and multidimensional Doppler method (MDM) use the instantaneous US signal phase (Sumi, 2002c, 2005c, 2008b). To measure a three-dimensional (3D) displacement vector (u_x,u_y,u_z), three or four 3D complex signals with different single-octant spectra (Fig. 1a reported by Sumi, 2008b) that extend analytic signals are calculated for respective echo data $r_1(x,y,z)$ and $r_2(x,y,z)$ obtained before and after a pulse repetition interval Δt, i.e., $r_{c1i}(x,y,z)$ and $r_{c2i}(x,y,z)$ [i = 1,..,3 or 1,..,4]. The multidimensional complex signal having single-orthant spectra was introduced by Hahn (1992) [1D complex signal phase and instantaneous frequency are specifically described in a literature by Bracewell (1986)].

Each 3D complex signal obtained has three instantaneous spatial frequencies, i.e., US frequency fx, lateral frequency fy and elevational frequency fz. Hereafter, (fx,fy,fz) is referred to as a frequency vector. When lateral and elevational modulations are performed, fy and fz are respectively the lateral and elevational modulation frequencies, whereas when lateral and elevational modulations are not performed (i.e., beam-steering is not performed), fy and fz are respectively yielded by synthesizing the lateral (Sumi 2002a, 2002c; Chen et al., 2004) and elevational phases (but, the frequencies are low and then the measurement accuracy is lower than that of LM [Sumi et al., 2010g; Sumi et al., 2010i; 2006c; Sumi & Shimizu, 20011]). Thus, as described next, an equation regarding with the unknown displacement vector (u_x,u_y,u_z) is derived from each pair of complex signals $r_{1ci}(x,y,z)$ and $r_{2ci}(x,y,z)$ having a same frequency vector (fx,fy,fz) [i = 1,..,3 or 1,..,4], and then the displacement vector (u_x,u_y,u_z) can be obtained by simultaneously solving the three or four independent equations having the independent vectors (fx,fy,fz) as the coefficients. The three equations can be arbitrary chosen from the four equations. To mitigate the calculation

errors of the instantaneous phases and frequencies, the least-squares method can also be used to solve all the four equations simultaneously.
Measuring a 2D displacement vector requires calculating two 2D complex signals with different single-quadrant spectra (Hahn, 1992) (Fig. 1b reported by Sumi, 2008i) and then solving two correspondingly derived simultaneous equations.

2.3 LCMs (Lateral Cosine Modulation Methods) using PAM, HAM and LGECM and optimizations

For respective PAM (Sumi, 2007d, 2008a, Sumi et al., 2008f, 2008i) and LGECM (Sumi, 2005c, 2008a, 2008b; Sumi et al., 2008f, 2008i) using a one-dimensional (1D) linear array-type transducer (lateral direction, y), the following apodization functions are used for the transmission or reception of US, i.e.,

$$\frac{1}{2\lambda x}\{\exp[-\frac{(2\pi)^2(\frac{y}{\lambda x}+f_y+f_a)^2(\frac{\sigma_y}{a})^2}{2}]+\exp[-\frac{(2\pi)^2(\frac{y}{\lambda x}-f_y-f_a)^2(\frac{\sigma_y}{a})^2}{2}]\} \quad (1)$$

and

$$\frac{1}{2\lambda x}\{[-\frac{4}{9}(\frac{\sigma_y}{a})^2\pi^2\left(\frac{y}{\lambda x}+f_y+f_a\right)^2+1]+[-\frac{4}{9}(\frac{\sigma_y}{a})^2\pi^2\left(\frac{y}{\lambda x}-f_y-f_a\right)^2+1]\}. \quad (2)$$

The apodization functions are superimpositions of two Gaussian functions and two parabolic functions. The apodization obtained for 20, 30, 60 and 100 mm depths are shown in Fig. 2 in the report by Sumi (2008b). HAM is also described by Sumi (2008i). These apodization functions are obtained using the Fraunhofer approximation such that the transmitted US energy used are same when realizing the Gaussian-type lateral PSF at a depth x for US with a wavelength λ, i.e.,

$$\exp(-\frac{y^2}{2\sigma_y^2})\cos(2\pi f_y y). \quad (3)$$

Here, f_y is the lateral modulation frequency and σ y corresponds to the lateral beam width for LGECM. f_a and a are parameters introduced to regulate lateral modulation frequency and bandwidth, respectively. For comparisons of FWHM and feet length, the Guassian and parabolic functions that have the same area are shown in Fig. 1c in the report by Sumi et al. (2008i).
The apodization functions for two-dimensional (2D) modulation (i.e., modulations in two directions y and z) using a 2D array-type transducer are also obtained for PAM and LGECM in a similar fashion (Sumi, 2005c; Sumi et al., 2008f, 2008i). According to the type of transducer (e.g., convex), other arbitrary orthogonal coordinates can also be used. When steered beams cannot be transmitted symmetrically in a lateral direction due to the existence of the obstacles such as a bone (for heart, liver etc), the original coordinate can be rotated such that the steered beams become laterally symmetric. However, our developed MCSPGM, MAM and MDM can yield measurement results even if the coordinate is not set in such a way, and the measurement accuracy in a displacement vector will be increased by the fact that the measurement accuracy of a lateral displacement can be significantly

improved (Sumi, 2010g; 2010i). Such a rotation also allows the use of our developed demodulation method with one of conventional 1D displacement measurement methods.
When carrying out PAM, HAM or LGECM, Methods 1 and 2 developed for transmission/reception focussing are used (Sumi, 2005c, 2007d, 2008a, 2008b; Sumi et al., 2008i, 2008f). The Methods used for LCM are also reviewed in this section. Both Methods 1 and 2 yield twofold lateral modulation frequency (Sumi, 2004, 2008b) compared with a method that performs only a receiving modulation, i.e., the method using a non-steered plane wave for a transmission with a rectangular window, Bingham window, Hanning window or Gaussian function as the apodization function (Jensen et al., 1998; Anderson, 1998. Also both Methods 1 and 2 enable decreases in effective aperture length (i.e., channels). When using LGECM method together with Method 1, the following PSF would be realized, i.e.,

$$\exp\left(-\frac{y^2}{2(\sigma_y/\sqrt{2})^2}\right)\cos\left[2\pi\left(2f_y\right)y\right]. \tag{4}$$

Different from Method 2, Method 1 also enables an increase in lateral bandwidth compared with the method that performs only a receiving modulation. For both methods, a low-frequency envelope signal must also be removed. By Basarab (2007), a twofold frequency sine modulation (i.e., not LCM) is carried out. However, the modulation is not appropriate for US imaging and measurement of displacement. This can be easily understood by assuming the existence of a point reflection target in the region of interest (ROI).
Method 1: (i) When a point of interest is dealt with, twofold frequency modulation can be performed using the same lateral modulation apodization (i.e., PAM) and spherical focusing in transmitting/receiving beam-forming as in conventional beam-forming (Sumi, 2004, 2008b). For 2D displacement vector measurement, two steered beams are used, whereas for 3D displacement vector measurement, three or four steered beams are used. These beams can be simulataneously transmitted. Alternatively, they can be superimposed after transmitting and receiving the respective beams successively. To obtain the steered beams, mechanical scans can also be performed. Plural transducers can also be used. When a finite ROI is dealt with, multiple transmitting modulations may also be useful for so-called multiple transmitting focusing. (ii) When performing a twofold frequency modulation over a finite ROI, the classical synthesis of an aperture (i.e., a monostatic or multistatic synthetic aperture) can also be carried out. However, if the target motion is rapid, a motional artifact may occur due to the low US energy transmitted from an element. In such a case, low-SNR echo modulation may be achieved. To increase the echo SNR, virtual sources can be used (e.g., Sumi and Uga, 2010h).
By performing a modulation using (i) or (ii), LGECM theoretically yields $\sqrt{2}$ times as wide a lateral bandwidth as that yielded by a method that performs only a receiving modulation (theoretically, the beam width becomes $\sigma y/\sqrt{2}$). Similarly, when performing other modulations such as PAM and HAM, an increase in lateral bandwidth is also achieved. Thus, using the same effective aperture width (i.e., the same number of channels), Method 1 realizes twofold lateral modulation frequency and a wide lateral bandwidth. The same lateral modulation frequency and lateral bandwidth can also be obtained by using a small effective aperture width (i.e., fewer channels).
Method 2: When dealing with a finite ROI, transmissions of steered two laterally wide plane waves that are realized simultaneously or successively with the same steering angles as those used in the receiving modulation can also be performed, of which apodizations are also properly performed. Although Method 2 cannot increase the lateral bandwidth, it is

useful because the measurement accuracies of MCSPGM, MAM, and MDM are more sensitive to US and modulation frequencies than the axial and lateral bandwidths, particularly when measuring a rigid motion (Sumi, 2008b). Method 2 realizes a more rapid echo modulation than Method 1. Thus, Method 2 is also robust against tissue motion during echo data acquisition. Similarly to Method 1, plural transducers can be used.

The combinations of PAM, HAM, and LGECM with Methods 1 and 2 are examined in reports by Sumi, 2007d, 2008a; Sumi et al., 2008i by simulations and agar phantom experiments. For all the combinations, by increasing the lateral modulation frequency (i.e., steering angles) to some extent, the echo SNR decreases due to improper beam-forming. For instance, when using a transducer for an agar phantom as that used in section 3, a modulation with the same frequency as that of US has a low echo SNR. The highest effective modulation frequency is determined by the US frequency and the transducer (e.g., element size). For the combinations, the echo SNRs were evaluated using the US echos, PSF values (see appendicies in reports by Sumi et al., 2008f, 2008i), or PSF energy (i.e., within a bandwidth). When using MAM for the phantom, the modulations at half the US frequency enabled accurate measurements of displacement vectors and elasticity, i.e., strain tensor and shear modulus. In addition, Methods 1 and 2 (i.e., twofold frequency modulations) yielded higher echo SNRs than the method that performs only receiving modulation, even if the same modulation frequency was realized by using a large effective aperture size and large steering angles.

Specifically, the order of echo SNRs obtained was PAM > LGECM when using Method 1 (Sumi, 2007d, 2008a; Sumi et al., 2008i). Moreover, PAM yields a wider lateral bandwidth than LGECM for the same effective aperture size. HAM yields almost the same results as LGECM, although the effective aperture size can be substantially decreased. As revealed in reports by Sumi, 2007d, 2008a, 2008b; Sumi et al., 2008i, compared with spherical focusing (Sumi, 2004), the use of plane waves decreases the achievable modulation frequency (Sumi, 2008b) and the echo SNR (Sumi, 2007d, 2008a; Sumi et al., 2008i). In addition, the use of plane waves also makes it difficult to deal with a deeply situated ROI. Thus, Method 1 yielded higher echo SNRs than Method 2 that uses two plane waves for transmission of US. However, in Method 2, the order of echo SNRs was inverted, i.e., LGECM > PAM (Sumi, 2007d, 2008a; Sumi et al., 2008i). This can be understood by considering the shapes of the apodization functions. The shape of the parabolic function is more similar to the rectangular function than to the Gaussian function (i.e., the Gaussian function has long feet, whereas the parabolic function has a wide main lobe).

To obtain a higher quality US image (i.e., an image with a high echo SNR and high or uniform spatial resolution) and to realize more accurate measurements of blood vector flow and elasticity, we have also conducted the determination of optimal beam-forming parameters as mentioned in section 1 (e.g., Sumi et al, 2006a, 2009c, 2010c; Sumi, 2007d, 2010a). For the optimization, the beam property of one element must be obtained in advance, analytically, numerically, or experimentally, as a function of the parameters. Because the synthesized US beam can be considered as a linear-weighted superimposition of the beams transmitted widely or received at the respective elements with suitable delays for focusing, we obtain simultaneous linear equations involving the unknown apodization function vector $\mathbf{x}$, a matrix $\mathbf{A}$ comprising the US beam values transmitted to an ROI from the respective elements of the US array, and a vector $\mathbf{b}$ comprising the designed PSF values in the ROI (i.e., $\mathbf{Ax} = \mathbf{b}$). However, because the independence of the rows of matrix $\mathbf{A}$ is low, the vector $\mathbf{x}$ must be determined stably by obtaining the inverse of $\mathbf{A}$ using singular-value

decomposition (SVD: Sumi, 2008d), a weighted minimum-norm least-squares solution (WMNLSQ: Sumi, 2007d, 2010a), regularization (Sumi, 2007d, 2010a) or nonlinear optimization (Sumi et al., 2009c). As far, a new analytic function that is expressed using a direct current and a power function divided has been obtained as the better PSF (Sumi et al., 2008g, 2009d, 2010c). The uses of the optimally determined apodization functions are beyond the scope of this paper.

2.4 MAM and MDM

Both the multidimensional autocorrelation method (MAM) and multidimensional Doppler method (MDM) use the instantaneous US signal phase (Sumi, 2002c, 2005c, 2008b). To measure a three-dimensional (3D) displacement vector (u_x,u_y,u_z), three or four 3D complex signals with different single-octant spectra that extend 1D analytic signal are calculated for echo data obtained before and after a pulse repetition interval Δt . The displacement vector (u_x,u_y,u_z) is obtained by solving the simultaneous equations (i.e., four or three independent equations) derived from the complex signals.

In MAM, an equation holds for the phase θ of each autocorrelation signal obtained from a pair of complex signals, i.e.,

$$\theta(0,0,0)+\frac{\partial}{\partial x}\theta(x,y,z)u_x+\frac{\partial}{\partial y}\theta(x,y,z)u_y+\frac{\partial}{\partial z}\theta(x,y,z)u_z=0. \tag{5}$$

Here, $\theta(0,0,0)$ equals the phase of the temporally or spatially moving-averaged lag one autocorrelation of the slow-time-axis signal sampled at the pulse repetition interval Δt [i.e., $\theta(0,0,0)$ is the moving-averaged instantaneous phase change that occurs during the pulse repetition interval Δt]. Moreover, $\partial/\partial x\ \theta$, $\partial/\partial y\ \theta$, and $\partial/\partial z\ \theta$ are the instantaneous spatial frequencies of the 3D echo signal, i.e., the US frequency fx (instantaneous frequency of the fast-time-axis signal sampled at the sampling interval of the AD converter), lateral frequency fy, and elevational frequency fz. The instantaneous spatial frequencies are estimated from the moving-averaged phase with spatial lags (x,y,z) by finite-difference approximation or differentiation using a differential filter with a cutoff frequency.

In MDM, an equation holds for the phase θ of each complex signal, i.e.,

$$\frac{\partial}{\partial t}\theta(x,y,z)\Delta t+\frac{\partial}{\partial x}\theta(x,y,z)u_x+\frac{\partial}{\partial y}\theta(x,y,z)u_y+\frac{\partial}{\partial z}\theta(x,y,z)u_z=0. \tag{6}$$

Here, $\partial/\partial t\ \theta\Delta t$ is the temporally or spatially moving-averaged instantaneous phase change that occurred during the pulse repetition interval Δt , and $\partial/\partial x\ \theta$, $\partial/\partial y\ \theta$ and $\partial/\partial z\ \theta$ are the instantaneous spatial frequencies of the 3D echo signal. The spatial and temporal derivatives can be obtained from the temporally or spatially moving-averaged instantaneous phase using the finite-difference approximation or a differential filter. $\partial/\partial t\ \theta\Delta t$ can also be obtained as the phase of the autocorrelation signal. Large displacements are dealt with by combining MCSPGM or MCCM.

When measuring a 2D displacement vector, two 2D complex signals with different single quadrant spectra are calculated, and the correspondingly derived simultaneous equations (i.e., two independent equations) are solved.

For respective MAM and MDM, by assuming a rigid motion locally, eqs. (5) and (6) can also be made simultaneously in the local region windowed to measure the motion as a local displacement vector (Sumi, 2002c, 2008b). The method obtained falls in a category of a block matching method such as MCSPGM and MCCM etc, these are respectively referred to as MAMb and MDMb (Sumi, 2002c, 2010g). However, through the simulations, their accuracies are significantly lower than those of the corresponding original methods. Then, these are not used now.

By Sumi (2008b), it was clarified by simulations that, for rigid motions, the order of the measurement accuracies of the displacement vectors is MAM > MDM for a high echo SNR and MDM > MAM for a low echo SNR. On deformed agar phantoms, when lateral modulations were not carried out, the order of the measurement accuracies of axial strains were the same as that for the high echo SNR (Sumi & Ebisawa, 2009a), whereas when using LGECM with Method 1, that of strain tensors was also same (Sumi et al., 2008i). Thus, although decorrelation noise generated due to target deformation also increased echo noise in the sense that pre- and post-deformation echo data were used, the laterally modulated echo data obtained by LGECM had a high SNR (Sumi, 2008b). Thus, in section 3, after showing, for the samely, laterally deformed agar phantom as that of previous reports (Sumi, 2008a, Sumi et al., 2008f, 2008i), US images and the corresponding 2D spectra laterally modulated with a half US frequency by PAM as well as LGECM using Methods 1 and 2, the measurement accuracies of MAM and MDM are also compared with each other.

3. Agar phantom experiments using PAM and LGECM with MAM and MDM

We have made a target agar phantom [40 (axial) × 96 (lateral) × 40 (elavational) mm^3] having a central circular cylindrical inclusion (diameter, 10 mm; depth, 19 mm) with a shear modulus different from that of the surrounding region, and shear moduli of 2.63 and 0.80 × 10^6 N/m^2 in the inclusion and surrounding regions, respectively (Sumi, 2008a, Sumi et al., 2008f, 2008i). Thus, the relative shear modulus was 3.29. Manually, the phantom was compressed by 2.0 mm in the lateral direction. The contact surfaces of the transducer and phantom were separated by immersing them in water in a tank, and a sponge was put under the phantom to allow the phantom to elongate in the axial direction by lateral uniform compression from the right-hand side using a large plate as in Case 1 in the experiments by Sumi (2007f). The left surface was fixed to a wall. A rectangular ROI 13.7 (axial, x) × 13.2 (lateral, y) mm^2 was centered on the inclusion (depths from 12.2 to 25.9 mm). For SA, Compaq Workstation DS20E (833 MHz) was used.

3.1 US imaging

Fig. 1 shows B-mode images for the ROI obtained by square detection for (a) nonmodulation (i.e., conventional beam-forming), (b) PAM with Method 1, (c) PAM with Method 2, (d) LGECMM with Method 1, and (e) LGECMM with Methos 2. The nominal frequency of US used was 7.5 MHz. The lateral modulation frequency was half the nominal frequency, i.e., 3.75 MHz [wavelengths, 0.408 vs axial 0.204 mm]. The lateral waves can be confirmed in Figs. 1(b) to 1(e). As shown, the lateral bandwidth of Fig. 1(b) is the largest. This can be confirmed by the lateral speckle sizes and specular echos (i.e., circled ones). Their lateral bandwidths can be more clearly compared in their 2D spectra in Figs. 2(a) to 2(e).

3.2 Elasticity measurement/imaging

Next, 2D shear modulus reconstructions (Sumi, 2005d) were performed together with 2D strain tensor measurements using the laterally modulated echo data obtained on the agar phantom (Figs. 1 and 2). For the 2D displacement vector measurement, MAM and MDM (Sumi, 2002c, 2005c, 2008b) were used (moving-average window size, 0.54 × 0.55 mm^2). For the coarse measurement, to prevent MAM and MDM from being subjected to aliasing in the evaluation of instantaneous phase due to the large lateral displacement (maximum, 2 mm), a 2D CCM was used (local window size, 0.54 × 2.15 mm^2). The local region size used was decreased when using MAM and MDM (Sumi et al., 1995d; Sumi, 1999a). After displacement vector measurements, 2D strain tensor components were obtained using a differential filter with a cutoff frequency of 0.89 mm^{-1}. For the 2D reconstruction, the method using a typical Poisson's ratio (0.5) was used under a 2D stress condition with regularization (Sumi, 2005d). Because the phantom was deformed primarily in the lateral direction, the reference region was set on the right borderline of the ROI. In addition, regularized 1D reconstruction (Sumi, 2005d, Sumi et al., 2007b) was also carried out using the principal lateral strain ε yy.

Table 1 shows the means and standard deviations obtained in a central square region having 5.5-mm-long sides in the inclusion for axial, lateral, and shear strains. By comparing the accuracies obtained by MAM and MDM, the order of echo SNRs is clarified to be the same as that reported by Sumi (2007d, 2008a, 2008i), i.e., inherent to the used beam-formings. This result arises because decorrelation noise generated due to the target deformation increases echo noise monotonically in the sense that pre- and post-deformation echo data are used. As the echo SNR decreases, the measurement errors in MAM and MDM increase. For instance, the SDs of the lateral strain ε yy measured by MAM are 0.28 (PAM with Method 1), 0.34 (LGECM and Method 1), 0.50 (LGECM and Method 2), and 0.72 (PAM and Method 2). In

	Strains			Shear moduli	
Methods	Axial (ϵ_{xx})	Lateral (ϵ_{yy})	Shear (ϵ_{xy})	2D	1D (Ratio of ϵ_{yy})
Parabolic -Method 1, MAM	0.01	-0.20	0.07	3.28	1.95
	(0.10)	(0.28)	(0.22)	(0.35)	(0.12)
MDM	0.01	-0.18	0.09	3.23	1.94
	(0.11)	(0.35)	(0.34)	(0.35)	(0.15)
-Method 2, MAM	0.005	-0.20	0.01	2.34	1.45
	(0.28)	(0.72)	(0.66)	(0.18)	(0.05)
MDM	0.003	-0.20	0.02	2.34	1.64
	(0.27)	(0.69)	(0.64)	(0.18)	(0.08)
Gaussian -Method 1, MAM	0.01	-0.22	0.06	3.14	1.85
	(0.13)	(0.34)	(0.24)	(0.32)	(0.13)
MDM	0.004	-0.22	0.08	3.17	1.89
	(0.14)	(0.36)	(0.30)	(0.33)	(0.15)
-Method 2, MAM	0.002	-0.21	0.03	2.60	1.94
	(0.21)	(0.50)	(0.44)	(0.22)	(0.12)
MDM	0.002	-0.22	0.04	2.63	1.69
	(0.21)	(0.45)	(0.45)	(0.22)	(0.09)

Table 1. For lateral modulation echo data obtained on agar phantom using listed methods, means and standard deviations (SDs in parentheses) evaluated for two-dimensional (2D) strain tensor measurement and 2D shear modulus reconstruction in central 5.5-mm-side square region of stiff inclusion (relative modulus 3.29). Results for 1D reconstructions obtained using lateral strain ratio are also shown.

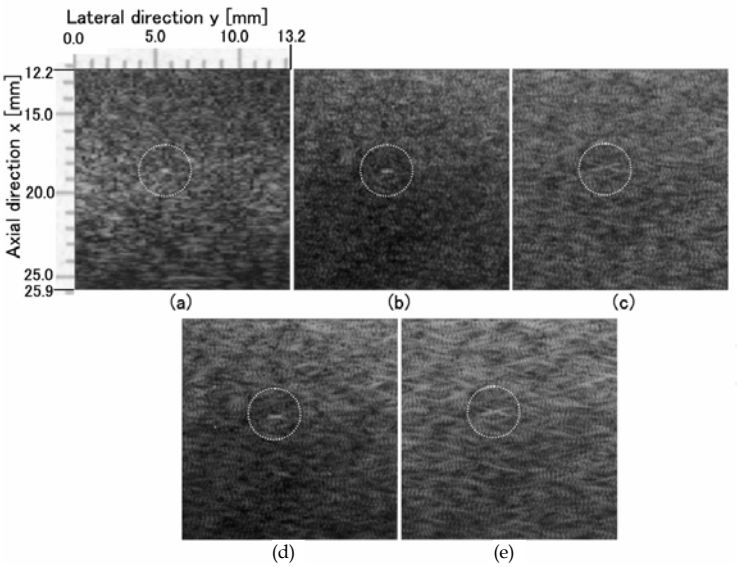

Fig. 1. B-mode images obtained using (a) no modulation; lateral cosine modulation (LCM), i.e., PAM with (b) Method 1 and (c) Method 2; LGECMM with (d) Method 1 and (e) Method 2. The specular echos from the same position are circled in the respective images.

the same manner, the order of the measurement accuracies of MAM and MDM became the same as that obtained in simulations for the rigid motion case (Sumi, 2008b). Specifically, for the lowest echo SNR obtained by PAM and Method 2, the order of accuracies of strain measurements is MDM > MAM, although large differences were not detected between their SDs; for instance, for lateral strain MDM became the same as that obtained in simulations for the rigid motion case: ε yy, 0.69 vs 0.72. For other modulations, the order of measurement accuracies is almost always MAM > MDM. In this case (Sumi, 2008b), the echo SNR obtained by PAM and Method 2 is low; that obtained by PAM and Method 1 is the highest of all. For the highest echo SNR, large differences were detected between the SDs; for example, for lateral strain ε yy, 0.28 vs 0.35.

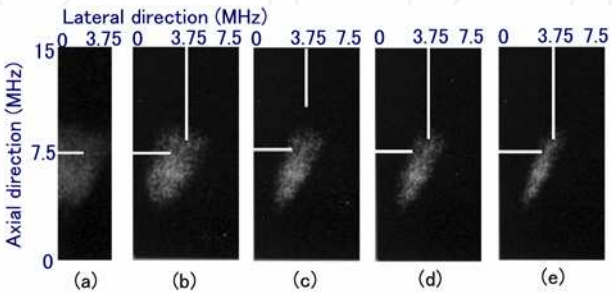

Fig. 2. 2D spectra for the ROI obtained from laterally modulated rf-echos corresponding to Figs. 1(a) to (e), i.e., (a) no modulation; lateral cosine modulation (LCM), i.e., PAM with (b) Method 1 and (c) Method 2; LGECMM with (d) Method 1 and (e) Method 2.

For visual comparison of the measurement accuracies, in Figs. 3 and 4 for the respective highest and lowest echo SNRs (i.e., PAM and Method 1, and PAM and Method 2), the lateral, axial, and shear strains ε yy, ε xx and ε xy measured using (a) MAM and (b) MDM are shown in a linear gray scale together with lateral and axial displacements dy and dx. As shown, for the highest echo SNR, both displacements dy and dx were stably measured by MAM [in Fig. 3(a)] and a circular stiff inclusion could be detected from the stably measured lateral and axial strain images. In the lateral strain image, the upper borderline of the inclusion was estimated to be quite soft. At the upper borderline of the inclusion, the inclusion and the surrounding region might be separated. However, in Figs. 3(b), 4(a), and 4(b), the effects due to the low echo SNRs and inherent to the displacement vector measurement methods can be visually confirmed in terms of the measured displacements and strains, particularly, in the lateral strain ε yy at the boundary of the circular stiff inclusion.

Next, 2D lateral shear modulus reconstructions are shown for all the combinations of PAM, LGECM, Methods 1 and 2, and MAM and MDM. The means and SDs of relative shear moduli obtained in the stiff inclusion are also summarized in Table 1, and for the highest and lowest echo SNRs, the log-gray-scaled reconstruction images are also shown in Figs. 3(a), 3(b), 4(a) and 4(b). For the highest echo SNR as well as other echo SNRs, the stiff circular region can be stably detected (LGECM data not shown). However, although for the highest echo SNR, the relative shear modulus was accurately reconstructed (the evaluated mean relative shear modulus, 3.28; SD, 0.35), the effects of strain measurement errors on the shear modulus reconstructions were confirmed, particularly from the mean shear moduli evaluated in the inclusion (Table 1). With increasing strain measurement error, the mean shear modulus decreased, i.e., for MAM, 3.28 (PAM and Method 1), 3.14 (LGECM and Method 1), 2.60 (LGECM and Method 2), 2.34 (PAM and Method 2); however, marked differences between the results obtained by MAM and MDM were not confirmed in this experiment, probably because of the proper smoothing achieved by the regularization (Sumi, 2005d).

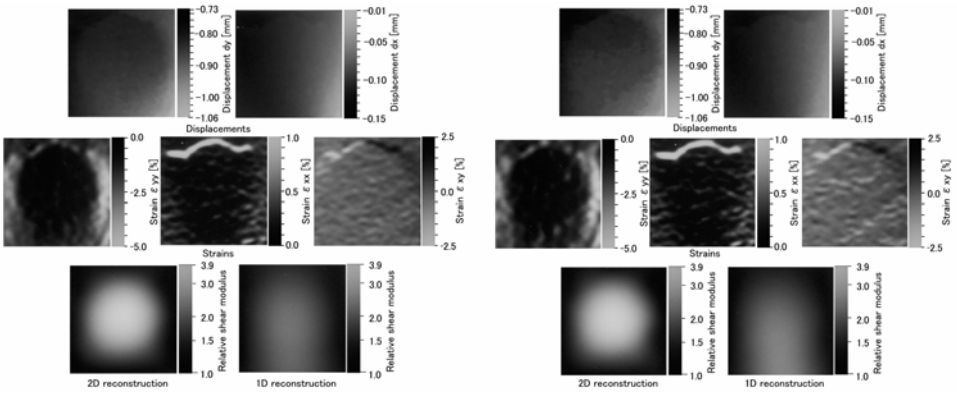

(a) (b)

Fig. 3. For the highest echo SNR obtained using PAM with Method 1 (lateral modulation frequency, 3.75 MHz vs US freq., 7.5 MHz), measured by (a) MAM and (b) MDM, i.e., lateral and axial displacements dy and dx, lateral, axial and shear strains ε yy, ε xx and ε xy, 2D shear modulus reconstruction and lateral 1D shear modulus reconstruction.

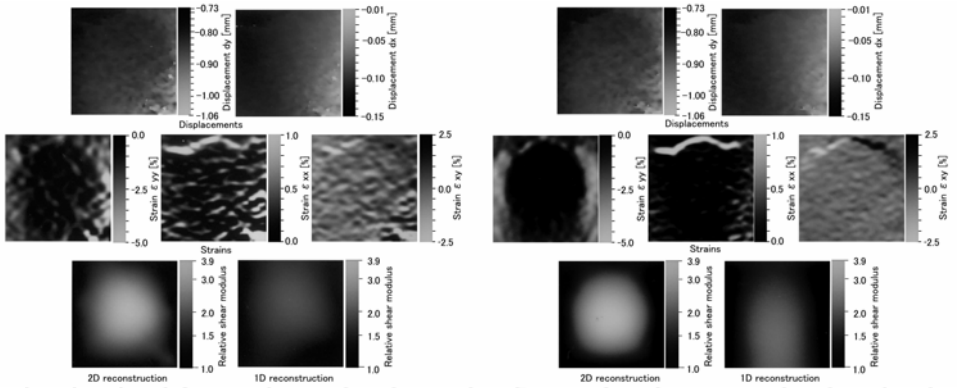

(a) (b)

Fig. 4. For the lowest echo SNR obtained using PAM with Method 2 (lateral modulation frequency, 3.75 MHz), measured by (a) MAM and (b) MDM. See captions of Fig. 3.

Furthermore, because the target phantom was deformed primarily in the lateral direction (Sumi, 2007f), the lateral 1D reconstruction might yield a useful shear modulus reconstruction, as was the case with the axial 1D reconstruction where the target was deformed primarily in the axial direction (Sumi, 2005d, 2007f). However, even for the highest echo SNR, as shown, the shape of the inclusion is not a circle. The phantom was not deformed horizontally, i.e., not accurately, in the lateral direction. The strains generated were small in the neighborhood of the lower borderline of the ROI. For the highest echo SNR, the mean relative shear modulus of the inclusion was 1.95 (SD, 0.12). This value lower than the original value is also affected by an artifact of the 1D reconstruction, i.e., the dynamic range of stiffness is estimated to be smaller than the original (Sumi, 2005d). For all the combinations, the means and SDs are shown in Table 1. Almost the same effects caused by strain measurement errors were confirmed as were confirmed in the 2D reconstructions.

4. Discussions and conclusions

In this report, we reviewed our several trials, searching for the best lateral modulation (i.e., coherent superimposition of echo signals) for US imaging with a high lateral resolution and accurate measurement of displacement vectors such as blood vector flow, a tissue displacement vector, a strain tensor, a strain rate tensor and an acceleration vector. PAM and HAM were introduced after LGECM to increase the echo SNR and lateral spatial resolution and decrease the effective aperture size. Such modulations were obtained on the basis of our knowledge about US propagation. The energy of the foot is lost during US propagation, and the main lobe contributes to the echo signals.

In the agar phantom experiment, PAM yielded a high echo SNR and a high lateral spatial resolution. Moreover, we compared the combinations of modulation methods and displacement vector measurement methods. Although for PAM, Method 1 yielded a more accurate 2D displacement vector/2D strain tensor than Method 2, in practical applications for *in vivo* tissues, rapid target motion will significantly affect the accuracy of Method 1. Because, a monostatic SA was used in this study, the echo SNR must be lower than that obtained when a conventional beam-former is used. In future studies, the limitations of Method 2 will also be

clarified such as obtaining of a high echo SNR in shorter time. A multistatic SA will also be reported. However, because large differences were not confirmed between MAM and MDM in this experiment, the echo data obtained by the monostatic SA had a rather high SNRs (Sumi, 2008b). If we can obtain a higher echo SNR, MAM will be more useful than MDM. Because MDM requires less calculation time than MAM (Sumi, 2008b), MDM may be better suited for 2D measurements of complex 3D blood flow and tissue motion and the 3D or 2D monitoring of various thermal treatments (Sumi, 2005d). Multiple transmitting modulations will also be performed. In future studies, the strain measurement accuracies of MAM and MDM will be clarified theoretically or through simulations or phantom experiments.

By using lateral deformation in the agar phantom experiment, we also obtained a meaningful result. The LCMs enable the attachment only of a US transducer to the target body in order to measure blood vector flow, the tissue strain tensor, and shear modulus reconstruction. In the axial strain measurement and 1D shear modulus reconstruction using the strain ratio (e.g., Sumi, 2005d, 2007f; Sumi & Matsuzawa, 2007b), the target must be compressed or elongated in the axial direction. Otherwise, the principle strain must be measured by setting the US beam in the direction of the target motion in successive scans (Sumi, 2010g). However, the LCMs enable freehand measurement and reconstruction in addition to dealing with uncontrollable target motion due to heart motion or pulsation and with deeply situated tissue that cannot be accessed from the body surface (e.g., liver and heart), although for the 2D measurements, a proper frame must be used to remove the out-of-motion from the frame. Recently, in addition to the reconstruction method used in this chapter [Method F referred to as in report by Sumi (2010d)], we have developed a shear modulus reconstruction method E from Methods F [Sumi et al., 1993, 1995a; Sumi, 1999c, 2005d, 2010d] and A to C [Sumi, 2006b, 2007g], which also enables the use of a quasi-reference shear modulus (quasi-reference value, e.g., unity) in order to obtain an accurate and unique shear modulus reconstruction in that the reconstruction has no geometrical artifacts, although the reconstruction has not absolute but relative shear modulus values (i.e., it depends on the quasi-reference value of shear modulus used) [Sumi, 2010d]. The use of a quasi-reference shear modulus enables us to deal with such deeply situated tissues. In Method F, when taking the logarithm of the shear modulus, an absolute or relative shear modulus reconstruction had been obtained as in this chapter; when not taking the logarithm and using a quasi-reference shear modulus, similarly an absolute or relative shear modulus reconstruction can also be obtained (Sumi et al., 1995a; Sumi, 2005d). Hereafter, all such relative reconstructions are referred to as those obtained by Method E (Sumi, 2010d).

In the experiment, accurate strain tensor measurements and shear modulus reconstructions were achieved, because we used the shear modulus reconstruction method F using a 2D stress assumption (Sumi, 2005d) and realized such a stress condition approximately. Thus, strictly speaking, the use of 2D US array will enable perfect measurement and reconstruction regardless of the direction of the dominant target motion. For tissue elasticity measurements, 3D shear modulus reconstruction should be performed with 3D displacement vector measurement. We have already developed six useful 3D shear modulus reconstruction methods, Methods F (Sumi et al., 1995a; Sumi, 1999c, 2005d, 2010d), A (Sumi, 2006b), B (Sumi, 2006b; 2007g), C (Sumi, 2007g), D (Sumi, 2008a, 2010d) and E (Sumi, 1999c, 2005d, 2010d), in which a finite difference method or a finite element method is properly used. Such 3D reconstruction can also be carried out in real-time as low-dimensional reconstruction (e.g., Sumi & Matsuzawa, 2007b) by setting a narrow 3D ROI even if a personal computer (PC) is used. The comparison of the methods will be reported elsewhere.

In this chapter, although we applied regularization only to the shear modulus reconstruction (Method F: Sumi, 2005d), its application to the displacement vector measurement, i.e., displacement component-dependent regularization or directional-dependent regularization (Sumi & Sato, 2008c; Sumi & Itoh, 2009b) will also be effective in stabilizing the strain tensor measurements by MAM, MDM, and MCSPGM in addition to shear modulus reconstruction. In both regularizations, the measured or theoretically predicted strain tensor variances are used to set the regularization parameters (Sumi & Sato, 2008c; Sumi, 2007a, 2008e; Sumi & Itoh, 2009b, 2010e). With such regularizations, a spatially varying regularization is also realized. As a result, the reconstructed shape of shear modulus inhomogeneity will be more improved.

We also referred to the determination of beam-forming parameters using optimization theory. Although we reported the use of analytic functions such as a parabolic function for PSF envelope, the better PSF has been obtained (Sumi et al., 2008g, 2009d, 2010c). The best PSF will also be sought in the same manner as the design of filters and windows. From the viewpoint of spatial resolution, PSF will be designed in the spatial and frequency domains. For echo SNR, knowledge of US propagation and decay is also required. By RanganathanIn & Walker (2003) and Guenther & Walker (2007), for conventional US imaging of a cyst, the contrast resolution is optimized by using a least squares estimation. In our case, target US properties such as a frequency-dependent attenuation will also be used in the determination of PSFs. Such a method of determination will be reported elsewhere together with the simultaneous determination of multiple parameters. Nonlinear optimization will also be used to determine a US element size and materials. Such an optimally realized PSF or laterally modulated PSF should also be used in US harmonic imaging and measurements as well as in radar (sumi, 2007d). These determinations may also reveal a new aspect of superresolution imaging by inverse filtering (Sumi et al., 2006a, 2008d, 2009c). For instance, in US imaging, a spatial resolution of less than 3mm is currently required to overcome the clinical limitations in conventional digital US imaging equipment (Sumi et al., 2008f; Sumi, 2010a).

Thus, an accurate real-time 3D US imaging, 3D tissue motion measurements (3D blood flow vector, tissue strain tensor, strain tensor rate etc.) and 3D shear modulus and viscoelasticity reconstructions (Sumi, 2005d, 2007d; Sumi et al., 2005a, 2008f, 2008i, 2009e) using a 2D US array will also be achieved. That is, the optimal determination of a 1D apodization function achieved can be easily extended to 2D functions (Sumi, 2008b). LCM makes it possible to attach an US transducer to the target body in order to achieve the measurements and reconstructions without considering the direction of the target motion. That is, being different from the 2D measurement, the LCM permits complete freehand measurements and reconstructions.

Optimal beamforming (LCM, etc.) can also enable the use of effective high intensity focused ultrasound (HIFU) with a high lateral resolution (Sumi, 2007d). Although the pulse shape and length of US must be considered technically, a proper high intensity US can also be used as a radiation force (ARF) [Bercoff et al., 2004; Dahl et al., 2007] for the imaging of shear waves or treatments. The use of a suitable receiver for HIFU and ARF will also be effective for diagnosis, monitoring and treatment (Sumi, 2002a, 2007d). The evaluation of the newly developed PSFs will also be performed by reconstruction of the mechanical source (e.g., Sumi et al., 2009e) or thermal source (e.g., Sumi et al., 2010b) using the proposed differential-type inverse methods. Thus, beamforming parameter determinations will also be used to develop a spatially uniform efficient and accurate treatment. A perfect minimum invasive

treatment will be also realized. Efforts will also be made to determine the high-frequency components in an apodization function for a very near field. A various *in vivo*/*in situ* microscope can also be realized using LM (e.g., skin: Sumi, 2008h; other applications such as a cultured cardiac cell: Sumi, 2009e; thermal properties: Sumi, 2010b).

In this chapter, we also reviewed MDSAM, MTM and thier applications (Sumi, 2002a, 2005d, 2008b). When small steering angles must be used, non-superimposition methods are more accurate than LCM (Sumi, 2008b). However, when realizing the modulation at half the US frequency as in the agar phantom experiment, the accuracies are almost the same (Sumi et al., 2008i). If we can achieve a higher lateral modulation frequency by realizing a more appropriate US transducer, LCM becomes more accurate than the non-superimposition methods. Moreover, such methods has the same problem as Method 1, and further requires accurate interpolations of the measured displacements at proper coordinates to evaluate the strain tensor.

By Sumi (2010g), a new more simple beamforming method was reported, i.e., ASTA referred to as by abbreviation of "a single steering angle." In conjunction, we also developed a new displacement vector measurement methods and lateral displacement measurement methods (Sumi, 2010g). For non-steered scanning, by rotating a coordinate when performing a beamforming or after obtaining a beam, a lateral frequncy can also be obtained. This is a version of ASTA. Thus, for instance, for the original and another version of ASTA, the application of MAM or MDM to an orthant spectra divided in a frequency domain also yields an accurate displacement vetor measurement (Sumi, 2010g; Sumi et al., 2010i). Also low frequency spectra can be disregared to increase a measurement accuracy of displacement (Sumi, 2010g; Sumi et al., 2010i). Although these methods are beyond the scope of this chapter, we briefly mention the problems of LM that can be coped with by ASTA (Sumi, 2010g), i.e.,

1. For a measurement in a 2D or 3D ROI, when a classical synthetic aperture (SA) is used, the US intensity transmitted from an element is small, which may yield low SNR echo data.
2. Alternatively, when crossed beams are superimposed, although a large US intensity can be obtained, time differences between the transmission of the beams can cause measurement errors, if the displacement occurs during these time differences.
3. If plural beams which have different paths are used, the inhomogeneity of tissue properties affects beamforming. Specifically, propagation speed affects focusing (i.e., the beam-crossing position), whereas attenuation and scattering lead to different frequencies of the crossed beams for the applications of 1D displacement measurement methods.
4. At the minimum, more time is required to complete a beamforming than that required with ASTA. Occasionally, more time is also required to complete a displacement calculation than is required with ASTA.
5. If obstacles such as bone exist in a superficial region, a deeply situated tissue cannot be dealt with, because a larger physical aperture is required than for conventional beamforming.

In contrast, with ASTA, although used for a displacement vector measurement, the number of available methods may be limited, and being dependent on the measurement method, only a lateral displacement measurement can be performed, and any of the above concerns, (1) to (5), will not become a problem, and a simple beamforming increases the number of applications of displacement measurement.

Because the highest quality and accuracy of imaging, measurement, and treatment should be spatially uniform, an optimization will also be performed under conditions in which transducers have physically finite effective aperture widths and various shapes. Thus, efforts to develop next-generation US diagnosis/treatment systems using proper beamforming and various methods of computational imaging are currently underway.

5. References

Anderson, M. E. (1998). Multi-dimensional velocity estimation with ultrasound using spatial quadrature. *IEEE Trans. Ultrason. Ferroelect. Freq. Contr.*, Vol. 45, No. 3, May 1998, pp. 852-861.

Anderson, M. E. (2000). A heterodyning demodulation technique for spatial quadrature. In: *Proceedings of the 2000 IEEE Ultrasonics Symposium*, p. 1487-1490, San-Juan, Oct 2000.

Basarab, A.; Gueth, P.; Liebgott, H.; Delachartre, P. (2007). Two-dimensional least-squares estimation for motion tracking in ultrasound elastography. In: *Proceedings of the 29th Ann. Int. Conf. IEEE Eng. Med. Biol. Soc.*, pp. 2155-2158, Lyon, Aug 2007.

Bercoff, J., Tanter, M., & Fink, M. (2004). Supersonic shear imaging: a new technique for soft tissue elasticitymapping. *IEEE Trans. Ultrason. Ferroelect. Freq. Contr.*, Vol. 51, No. 4, April 2004, pp. 396–409.

Bracewell, R. N. (1986). The Fourier transform and its applications. McGraw-Hill, New York

Bohs, L. N. & Trahey, G. E. (1991). A novel method for angle independent ultrasonic imaging of blood flow and tissue motion. *IEEE Trans. on Biomed. Eng.*, Vol. 38, No. 3, Mar 1991, pp. 280-286.

Cespedes, I.; Ophir, J.; Ponnekanti, H. & Maklad, N. F. (1993). Elastography: elasticity imaging using ultrasound with application to muscle and breast *in vivo* ultrasound imaging. *Ultrason. Imag.*, Vol. 15, No. 2, Apr 1993, pp. 73-88.

Chen, X.; Zohdy, M. J.; Emelianov, S. Y. & O'Donnell, M. (2004). Lateral speckle tracking using synthetic lateral phase. *IEEE Trans. Ultrason. Ferroelect. Freq. Contr.*, Vol. 51, No. 5, May 2005, pp. 540-550.

Dahl, J. J., Pinton, G. F., Palmeri, M. L., Agrawal, V., Nightingale, K. R., & Trahey, G. E. (2007). A parallel tracking method for acoustic radiation force impulse imaging. *IEEE Trans. Ultrason. Ferroelect. Freq. Contr.*, Vol. 54, No. 2, Feb 2007, pp. 301–311.

Doyley, M. M.; Srinivasa, S.; Pendergrass, S. A.; Wu, Z. & Ophir, J. (2005). Comparative evaluation of strain-based and model-based modulus elastography. *Ultrasound Med. Biol.*, Vol. 31, No. 6, Jun 2005, pp. 787-802.

Fox, M. D. (1978). Multiple crossed-beam ultrasound Doppler velocimetry. *IEEE Trans. on Sonics and Ultrasonics*, Vol. 25, No. 5, Sep 1978, pp. 281-286.

Garra, B. S., Cespedes, E. I. & Ophir, J. (1997). Elastography of breast lesions: initial clinical results. *Radiology*, Vol. 202, No. 1, Jan 1997, pp. 79–86.

Goodman, J. W. (1996). *Introduction to Fourier optics* (2nd ed). McGRAW-HILL COMPANIES, INC, New York.

Guenther, D. A. & Walker, W. F. (2007). Optimal apodization design for medical ultrasound using constrained least squares—part I: theory. *IEEE Trans. Ultrason. Ferroelect. Freq. Contr.*, Vol. 54, No. 2, Feb 2007, pp. 332–341.

Hahn, S. L. (1992). Multidimensional complex signals with single-orthant spectra. *Proc. IEEE*, Vol. 80, No. 8, Aug 1992, pp. 1287-1300.

Jensen, J. A. & Munk, P.(1998). A new method for estimation of velocity vectors. *IEEE Trans. Ultrason. Ferroelect. Freq. Contr.*, Vol. 45, No. 3, May 1998, pp. 837-851.

Jensen, J A. (2001). A new estimator for vector velocity estimation. *IEEE Trans. Ultrason. Ferroelect. Freq. Contr.*, Vol. 48, No. 4, Jul 2001, pp. 886-894.

Kallel, F. & Bertrand, M. (1996). Tissue elasticity reconstruction using linear perturbation method. *IEEE Trans. on Med. Imag.*, Vol. 15, No. 3, Jun 1996, pp. 299-313.

Kasai, C.; Namekawa, K.; Koyano, A. & Omoto, R. (1985). Real-time two-dimensional blood flow imaging using an autocorrelation technique. *IEEE Trans. on Sonics Ultrason.*, Vol. 32, No. 3, May 1985, pp. 458-464.

Liebgott, H.; Fromageau, J.; Wilhjelm, J. E.; Vray, D. & Delachartre, P. (2005). Beamforming scheme for 2D displacement estimation in ultrasound imaging. *EURASIP Journal on Applied Signal Processing*, Vol. 8, 2005, pp. 1212-1220.

Loupas, T.; Pomers, J.T. & Gill R.W. (1995). An axial velocity estimator for ultrasound blood flow imaging, based on a full evaluation of the Doppler equation by means of a two-dimensional autocorrelation method approach. IEEE Trans. Ultrasound Ferroelect., Freq. Contr., Vol. 42., No 4, Jully 1995, pp. 672-688.

Newhouse, V. L.; Censor, D.; Vontz, T.; Cisneros, J. A. & Goldberg, B. B. (1987). Ultrasound Doppler probing of flows transverse with respect to beam axis. *IEEE Trans. on Biomed. Eng.*, Vol. 34, No. 10, Oct 1987, pp. 779-789.

Ophir, J., Cespedes, I., Ponnekanti, H., Yazdi, Y. & Li, X. (1991). Elastography: a quantitative method for measuring the elasticity of biological tissues. *Ultrason Imaging*, Vol. 13, No. 2, Apr 1991, pp. 111-134.

Plewes, D. B.; Bishop, J.; Samani, A. & Sciarretta, J. (2000). Visualization and quantification of breast cancer biomechanical properties with magnetic resonance elastography. *Phys. Med. Biol.*, Vol. 45, No. 6, Jun 2000, pp. 1591-1610.

Ranganathan, K. & Walker, W. F. (2003). A novel beamformer design method for medical ultrasound—part I: theory. *IEEE Trans. Ultrason. Ferroelect. Freq. Contr.*, Vol. 50, No. 1, Jan 2003, pp. 15–24.

Srinivasan, S.; Kallel, F.; Souchon, R. & Ophir, J. (2002). Analysis of an adaptive strain estimation technique in Elastography. *Ultrasonic imaging*, Vol. 24, No. 2, Apr 2002, pp. 109-118.

Steinberg, B. D. (1976). *Principles of aperture & array system design*. John Wiley & Sons, Inc., New York.

Sumi, C.; Suzuki, A. & Nakayama, K. (1993). Estimation of shear modulus distribution in soft tissue from strain measurement. *Jpn. J. Med. Electr. Biol. Eng.*, Vol. 31(suppl.), p. 390, Koufu, May 1993 (in Japanese).

Sumi, C.; Suzuki, A.; Nakayama, K. (1994a). Estimation of shear modulus distribution in soft tissue from strain measurement. *Jpn. J. Med. Electr. Biol. Eng.*, Vol. 32(suppl.), p. 122, Takamatsu, May 1994.

Sumi, C.; Suzuki, A. & Nakayama, K. (1994b). Phantom experiment on reconstruction of shear modulus distribution in soft tissue from strain measurement. *Ultrasound in Medicine and Biology*, Vol. 20(Suppl 1: Proceedings of the *7th Congress of World Federation for Ultrasound in Medicine and Biology*), p. 14-4, Sapporo, July 1994.

Sumi, C.; Suzuki, A. & Nakayama, K. (1995a). Estimation of shear modulus distribution in soft tissue from strain distribution. *IEEE Trans. on Biomed. Eng.*, Vol. 42, No. 2, Feb 1995, pp. 193-202.

Sumi, C.; Suzuki, A.; Nakayama, K. & Kubota, K. (1995b). Estimation of stiffness distribution in soft tissue from displacement vector measurement. *Jpn. J. Med. Ultrasonics*, Vol. 22(suppl I), pp. 44, May 1995 (in Japanese).

Sumi, C.; Suzuki, A. & Nakayama, K. (1995c). Estimation of hardness distribution in soft tissue from strain ratio. *Jpn. J. Med. Ultrasonics*, Vol. 22(suppl II), p. 258, Nov 1995 (in Japanese).

Sumi, C.; Suzuki, A. & Nakayama, K. (1995d). Phantom experiment on estimation of shear modulus distribution in soft tissue from ultrasonic measurement of displacement vector field. *IEICE Trans. on Fundamental*, Vol. E78-A, No. 12, Dec 1995, pp. 1655-1664.

Sumi, C.; Suzuki, A. & Nakayama, K. (1996). Estimation of static elasticity distribution in living tissues from ultrasonic measurement of strain distributions. *Jpn. J. Med. Electr. Biol. Eng.*, Vol. 34(suppl.), p. 107, Osaka, May 1996 (in Japanese).

Sumi, C.; Nakayama, K.; Kubota, M. (1997). Tissue elasticity imaging based on ultrasonic strain measurement. *Jpn. J. Med. Electr. Biol. Eng.*, Vol. 35(suppl.), p. 171, Nagano, Apr 1997 (in Japanese).

Sumi, C. & Nakayama, K. (1998). A robust numerical solution to reconstruct a globally relative shear modulus distribution from strain measurements. *IEEE Trans. on Med. Imag.*, Vol. 17, No. 3, Jun 1998, pp. 419-428.

Sumi, C. (1999a). Fine elasticity imaging on utilizing the iterative rf-echo phase matching method. *IEEE Trans. Ultrason. Ferroelect. Freq. Contr.*, Vol. 46, No. 1, Jan 1999, pp. 158-166.

Sumi, C.; Shibata, K. & Kubota, M. (1999b). Shear modulus imaging of breast tissues. *Tech. Report of Jpn. Soc. of Ultrason. in Med.*, Vol. BT98, No. 4, pp. 28-31, Tokyo, Mar 1999 (in Japanese).

Sumi, C. (1999c). Toward 3-D reconstruction/imaging shear modulus distribution in living soft tissues. In: *Proceedings of Autumn Meeting Acoust. Soc. Japan*, pp. 1201–1202, Shimane, Sep 1999 (in Japanese).

Sumi, C., Ichiki, Y., Kanai, H. (2000a). Feasibility of monitoring thermal therapy by ultrasonic strain measurement-based shear modulus reconstruction. *Jpn. J. Med. Elect. And Biol. Eng.*, Vol. 38(suppl. I), p. 284, May 2000 (in Japanease).

Sumi, C., Nakayama, K. & Kubota, M. (2000b). An effective ultrasonic strain measurement-based shear modulus reconstruction technique for superficial tissues – Demonstration on in vitro pork ribs and in vivo human breast tissues. *Phys. in Med. Biol.*, Vol. 45, No. 6, June 2000, pp. 1511-1520.

Sumi, C.; Takegahara, S. & Kanai, H. (2001a). Feasibility of shear modulus imaging technique for monitoring the effectiveness of the interstitial RF electromagnetic wave thermal therapy. In: *Proceedings of SPIE*, Vol. 4247, pp. 151-157, San Jose, Jan 2001.

Sumi, C & Kojima, R. (2001b). Quantitative evaluation of effectiveness of thermal therapy through shear modulus reconstruction on utilization of interstitial RF electromagnetic wave thermal applicator system. Vol. BT2000, pp. 21-28, Mar 2001 (in Japanese).

Sumi, C. (2002a). Displacement measurement method and apparatus, strain measurement method and apparatus, elasticity and viscoelasticity constants measurement apparatus, and the elasticity and viscoelasticity constants measurement apparatus based treatment apparatus. Japanese Patent 4260523, Apr 30, 2009 (application Apr

25, 2002); US Patent US 7,775,980 B2, Aug 17, 2010 (application 10/326,526, Dec 23, 2002).

Sumi, C. (2002b). Realization of combined diagnosis/treatment style by ultrasonic strain measurement-based mechanical properties imaging technique - examples with applications on the interstitial rf-electromagnetic wave thermal therapy. *Abstracts of First International Conference of Ultrasonic Measurement and Imaging of Tissue Elasticity*, p. 23, Niagara-Falls, October 2002.

Sumi, C. (2002c). Digital measurement method of tissue displacement vector from instantaneous phase of ultrasonic echo signal. *Technical report of Japn. Soc. of Ultrason. in Med.*, Vol. 102, No. 4, pp. 37-40, Fukuoka, December 2002.

Sumi, C. (2004). Improvement of measurement accuracy of displacement vector by lateral modulation. In: *Proceedings of the 2004 Autumn Meeting of the Acoustical Society of Japan*, pp. 1353–1354, September 2004 (in Japanese).

Sumi, C.; Kubota, M.; Wakabayashi, G.; & Tanabe, M. (2005a). Usefulness of ultrasonic strain measurement-based mechanical properties imaging technique: Toward realization of short-time diagnosis/treatment, In: *Research and Development in Breast Ultrasound* eds by Ueno, E., Shiina, T., Kubota, M. & Sawai, K., pp. 16-43, Springer, New York.

Sumi, C. (2005b). Real-time reconstruction of shear modulus distribution by calculating strain ratio. In: *Proceedings of 27th Ann. Int. Conf. of IEEE Eng. in Med. Biol. Soc.*, CD-ROM, Shnaghai, September 2005.

Sumi, C. (2005c). Multidimensional displacement vector measurement methods utilizing instantaneous phase. In: *Proceedings of 27th Int. Conf. of IEEE Eng. of Med. and Biol. Soc.*, CD-ROM, Shanghai, September 2005.

Sumi, C. (2005d). Usefulness of ultrasonic strain measurement-based shear modulus reconstruction for diagnosis and thermal treatment. *IEEE Trans. Ultrason. Ferroelect. Freq. Contr.*, Vol. 52, No. 10, Oct 2005, pp. 1670-1689.

Sumi, C. & Noro, T. (2006a). Lateral Gaussian envelope cosine modulation method (LGECMM) (4th report)—a breakaway from Fraunhofer approximation, In: *Proceedings of the Autumn Meeting of the Acoustical Society of Japan*, pp. 1035–1036, Sep 2006.

Sumi, C. (2006b). Reconstructions of shear modulus, Poisson's ratio and density using approximate mean normal stress $\lambda\varepsilon_{\alpha\alpha}$ as unknown. *IEEE Trans. Ultrason. Ferroelect. Freq. Contr.*, Vol. 53, No. 12, Dec 2006, pp. 2416-2434.

Sumi, C.; Kikuchi, D.; Shimada, Y.; Nojiri, S. (2006c). Comparison of multidimensional shear modules reconstruction methods through simulations and phantom experiments. Abstract of fifth International Conference of Ultrasonic Measurement and Imaging of Tissue Elasticity, p. 139, Utah, October 2006.

Sumi, C. (2007a). Spatially variant regularization for tissue strain measurement and shear modulus reconstruction. *Journal of Medical Ultrasound*, Vol. 34, No. 3, Sep 2007, pp. 125-131.

Sumi, C. & Matsuzawa, H. (2007b). Shear modulus reconstruction by ultrasonically measured strain ratio. *Journal of Medical Ultrasonics*, Vol. 34, No. 4, Dec 2007, pp. 171-188.

Sumi, C. & Sato, K. (2007c). Evaluation of variances of ultrasonically measured strain tensor components. *Acoustical Science and Technology*, Vol. 28, No. 5, Sep 2007, pp. 352-356.

Sumi, C. (2007d). Beamforming for realizing designed point spread function, In: *Proceedings of IEEE Ultrasonics Symposium*, pp. 1557–1562, New York, Oct 2007.

Sumi, C.; Tanuma, A.; Itoh, T. & Takahashi, D. (2007e) Effectiveness of regularization and lateral modulation on multidimensional shear modulus reconstruction in displacement vector measurement.. In: *Proceedings of the sixth International Conference on the Ultrasonic Measurement and Imaging of Tissue Elasticity*, Santa Fe, p. 90, Oct 2007.

Sumi, C. (2007f). Ultrasonic axial strain measurement for lateral tissue deformation. *Ultrasound Med. Biol.*, Vol. 33, No. 11, Nov 2007, pp. 1830-1837.

Sumi, C. (2007g). Effective shear modulus reconstruction obtained with approximate mean normal stress remaining unknown. *IEEE Trans. Ultrason. Ferroelect. Freq. Contr.*, Vol. 54, No. 11, Nov 2007, pp. 2394-2403.

Sumi, C. (2008a). Increasing accuracy of tissue shear modulus reconstruction using ultrasonic strain tensor measurement – Regularization and lateral modulation," In: *Acoustical Im*aging (Vol. 29) ed by Akiyama I., pp. 59-69, Springer.

Sumi, C. (2008b). Displacement vector measurement using instantaneous ultrasound signal phase —Multidimensional autocorrelation and Doppler methods" *IEEE Trans. Ultrason. Ferroelect. Freq. Contr.*, Vol. 55, No. 1, Jan 2008, pp. 24-43.

Sumi, C. & Sato, K. (2008c). Regularization for ultrasonic measurements of tissue displacement vector and strain tensor. *IEEE Trans. Ultrason. Ferroelect. Freq. Contr.*, Vol. 55, No. 2, Feb 2008, pp. 787-799.

Sumi, C. (2008d). A case of apodization function using singular value decomposition: Determination of beamforming parameters by optimization. *Acoustical Science and Technology*, Vol. 29, No. 2, Mar 2008, pp. 185-187.

Sumi, C. (2008e). Regularization of tissue shear modulus reconstruction using strain variance. *IEEE Trans. Ultrason. Ferroelect. Freq. Contr.*, Vol. 55, No. 4, Apr 2008, pp. 297-307.

Sumi, C. & Tanuma, A. (2008f). Comparison of parabolic and Gaussian lateral cosine modulations in ultrasound imaging, displacement vector measurement, and elasticity measurement. *Jpn, J. Appl. Phys.*, Vol. 47, No. 5B, May 2008, pp. 4137-4144.

Sumi, C.; Komiya, Y. & Uga, S. (2008g). Proper point spread function for lateral modulation. In: *Proceedings of the 7th International Conference on Ultrasonic Measurement and Imaging of Tissue Elasticity*, Austin, Oct 2008 (6 pages).

Sumi, C. & Saijo, Y. (2008h). Shear modulus microscopy using displacement vector measurement, In: *Proceeding version of the seventh International Conference on the Ultrasonic Measurement and Imaging of Tissue Elasticity*, Austin, Oct 2008 (5 pages).

Sumi, C.; Noro, T.; Tanuma, A. (2008i). Effective lateral modulations with applications to shear modulus reconstruction using displacement vector measurement. *IEEE Trans. Ultrason. Ferroelect. Freq. Contr.*, Vol. 55, No. 12, Dec 2008, pp. 2607-2625.

Sumi, C. & Ebisawa, T. (2009a). Phantom experiments of axial strain measurements using multidimensional autocorrelation method, multidimensional Doppler method and direct strain measurement method. *Acoustical Science and Technology*, Vol. 30, No. 2, Mar 2009, pp. 117-123.

Sumi, C. & Itoh, T. (2009b). Spatially variant regularization of lateral displacement measurement using variance. *Ultrasonics*, Vol. 49, No. 4-5, May 2009, pp. 459-465.

Sumi, C.; Komiya, Y. & Uga, S. (2009c). A demonstration of optimal apodization determination for proper lateral modulation. *Jpn, J. Appl. Phys.*, Vol. 48, No. 7B, Jul 2009, 07GJ06 (10 pages).

Sumi, C.; Shimizu, K.; Takanashi, Y.; Tadokoro, Y. & Nozaki, Y. (2009d). 2nd report on proper point spread function for lateral modulation. In: *Proceedings of the 8th*

International Conference on Ultrasonic Measurement and Imaging of Tissue Elasticity, Vlissingen, Sep 2009 (3 pages).

Sumi, C. & Suekane S. (2009e). Reconstruction of a tissue shear modulus together with mechanical sources. *Therm. Med.*, Vol. 25, No. 4, Dec 2009, pp. 89-104.

Sumi, C. (2010a). Determination of lateral modulation apodization functions using a regularized, weighted least squares estimation. *Int. J. Biomed. Imag*, Mar 2010, ID635294 (7 pages).

Sumi, C.; Kanada, H. & Takanashi, Y. (2010b). Reconstructions of tissue thermal properties together with perfusion and thermal source. *Thermal Medicine*, Vol. 26, No. 1, Mar 2010, pp. 31–40.

Sumi, C.; Shimizu, K. & Matsui, N. (2010c). Proper analytic point spread function for lateral modulation. *Jpn J Appl Phys*, Vol. 49, No. 7B, Jul 2010, 07HF07 (2 pages).

Sumi, C. (2010d). Relative shear modulus reconstruction for visualization with no geometrical artifact. *Acoustical Science and Technology*, Vol. 31, No. 5, Sep 2010, pp. 347-359.

Sumi, C. & Itoh, T. (2010e). A limitation in use of spatially stationary strain variance estimate in regularization of shear modulus reconstruction. *Acoustical Science and Technology*, Vol. 31, No. 5, Sep 2010, pp. 360-367.

Sumi, C.; Takanashi, Y.; Shimizu, K. & Ishii, Y. (2010f). Determining if the relative shear modulus or the inverse of the relative shear modulus should be imaged using axial strain ratios on agar phantoms. *Ultrasound Med. Biol.*, Vol. 36, No. 9, Sep 2010, pp. 1481-1491.

Sumi, C. (2010g). Utilization of an ultrasound beam steering angle. *Reports in Medical Imaging*, Vol. 3, Sep 2010, pp. 61-81.

Sumi, C. & Uga, S. (2010h). Effective ultrasonic virtual sources which can be positioned independently of physical aperture focus positions. *Reports in Medical Imaging*, Vol. 3, Sep 2010, pp. 45-59.

Sumi, C., Shimizu, K., Takanashi, Y. (2010i). Increase in spatial resolution of lateral modulation imaging. In: *Proceeding version of the nineth International Conference on the Ultrasonic Measurement and Imaging of Tissue Elasticity*, Utah, Oct 2010 (in press).

Sumi, C. & Shimizu, K. (2011). Agar phantom experiment for comparison of measurement accuracy of tissue elasticity obtained by displacement vector measurement using lateral modulation with multidimensional autocorrelation and Doppler methods and corresponding one-dimensional methods. Jpn. J. Appl. Phys. (submitted).

Tanter, M.; Bercoff, J.; Sandrin, L. & Fink, M. (2002). Ultrafast compound imaging for 2-D motion vector estimation: application to transient Elastography. *IEEE Trans. Ultrason. Ferroelect. Freq. Contr.*, Vol. 49, No. 10, Oct 2002, pp. 1363–1374.

Techavipoo, U.; Chen, Q.; Varghese, T.; Zagzebski, J. A. (2004). Estimation of displacement vectors and strain tensors in elastography using angular isonifications. *IEEE Trans Med. Imag.*, Vol. 23, No. 12, Dec 2004, pp. 1479–1489.

Wilson, L. S. & Robinson, D. E. (1982). Ultrasonic measurement of small displacements and deformations of tissue. *Ultrason. Imaging*, Vol. 4, No. 1, Jan 1982, pp. 71-82.

Yagi, S. & Nakayama, K. (1988). Local displacement analysis of inhomogeneous soft tissue by spatial correlation of rf echo signals. In: *Proceedings of WFUMB Meeting,* p. 113, Washington DC, 1988.

Yamakawa, M. & Shiina, T. (2001). Strain estimation using the extended combined autocorrelation method. *Jpn. J. Appl. Phys.*, Vol. 40(Part 1), No. 5B, May 2001, pp. 3872–3876.

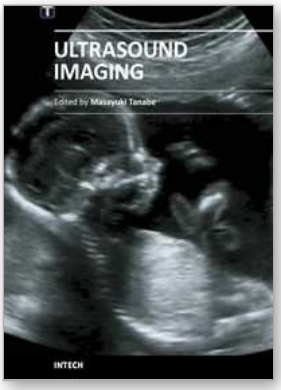

Ultrasound Imaging

Edited by Mr Masayuki Tanabe

ISBN 978-953-307-239-5
Hard cover, 210 pages
Publisher InTech
Published online 11, April, 2011
Published in print edition April, 2011

In this book, we present a dozen state of the art developments for ultrasound imaging, for example, hardware implementation, transducer, beamforming, signal processing, measurement of elasticity and diagnosis. The editors would like to thank all the chapter authors, who focused on the publication of this book.

How to reference

In order to correctly reference this scholarly work, feel free to copy and paste the following:

Chikayoshi Sumi (2011). Ultrasonic Measurement and Imaging with Lateral Modulation – Echo, Tissue Motion and Elasticity, Ultrasound Imaging, Mr Masayuki Tanabe (Ed.), ISBN: 978-953-307-239-5, InTech, Available from: http://www.intechopen.com/books/ultrasound-imaging/ultrasonic-measurement-and-imaging-with-lateral-modulation-echo-tissue-motion-and-elasticity

INTECH
open science | open minds

InTech Europe
University Campus STeP Ri
Slavka Krautzeka 83/A
51000 Rijeka, Croatia
Phone: +385 (51) 770 447
Fax: +385 (51) 686 166
www.intechopen.com

InTech China
Unit 405, Office Block, Hotel Equatorial Shanghai
No.65, Yan An Road (West), Shanghai, 200040, China
中国上海市延安西路65号上海国际贵都大饭店办公楼405单元
Phone: +86-21-62489820
Fax: +86-21-62489821